Chapter 3

Degradation of Black Phosphorus upon Environmental Exposure and Encapsulation Strategies To Prevent It

Yu Kyoung Ryu,* Andres Castellanos-Gomez, and Riccardo Frisenda

Materials Science Factory, Instituto de Ciencia de Materiales de Madrid(ICMM-CSIC), Madrid E-28049, Spain

***E-mail: yukyoung.ryu@csic.es.**

Along this chapter we discuss about one of the main issues in black phosphorus research: its environmental instability. We will discuss the works were the role of the environmental exposure has been studied and the reported works describing strategies to effectively encapsulate black phosphorus to preserve its pristine properties.

Introduction

In 2013, Yuanbo Zhang and co-workers demonstrated that graphene was not the only elemental two-dimensional material that could be isolated by exfoliation of a bulk layered crystal (*1*). Atomically thin layers, and even one-atom thick layers, of phosphorus can be isolated by mechanical and chemical exfoliation of bulk black phosphorus, a stable layered allotrope of phosphorus, crystals. Bridgman grew black phosphorus single crystals for the first time in 1914. He was investigating phase transformations of white phosphorus under high pressure and discover the black phosphorus allotrope by serendipity. In his original manuscript Bridgman said: "*…Black phosphorus was discovered during an attempt to force ordinary white phosphorus to change into red phosphorus by the application of high hydrostatic pressure…*" (*2*).

Regarding the optical and electronic properties of black phosphorus, in bulk it is a semiconductor with a direct bandgap of 0.35 eV and charge carrier mobilities in the order of 10000 $cm^2/V{\cdot}s$ (*3*). Thin flakes of black phosphorus have been recently used in field-effect transistors (FETs) showing mobility values up to 1000 $cm^2/V{\cdot}s$ (*4–6*) at room temperature and up to ~4000 $cm^2/V{\cdot}s$ at low temperatures (*7–9*). Moreover, due to its small and direct bandgap black phosphorus has a bright perspective for broadband photodetection where transition metal dichalcogenides are limited because of their large bandgap (*10–16*).

Unlike other 2D materials isolated to date, however, black phosphorus is rather environmentally instable. Therefore, the attainment of either stable thin layers or effective passivation methods is required to produce reliable BP-based optoelectronic devices (*17–19*). In the following we will

Ji; Fundamentals and Applications of Phosphorus Nanomaterials
ACS Symposium Series; American Chemical Society: Washington, DC, 2019.

discuss about this issue and about the strategies developed to overcome this environmental instability.

Origin of the Instability under Ambient Conditions

Most of the two-dimensional materials isolated prior to 2014 (graphene, h-BN, MoS_2, etc…) are rather stable at atmospheric conditions which facilitated the fabrication of devices based on these materials. Black phosphorus, however, shows a relatively large reactivity (*20*, *21*). This reactivity is originated by its particular puckered honeycomb crystal structure. In black phosphorus, the phosphorus atoms have 5 valence shell electrons available for bonding with a valence shell configuration $3s^2 3p^3$. Therefore, each phosphorus atom bonds to three neighboring phosphorus atoms through sp^3 hybridized orbitals, making the phosphorus atoms to form a puckered honeycomb lattice (orthorhombic, with space group *Cmca*) and each phosphorus atom also has a lone pair (a pair of valence electrons that are not shared with another neighbouring atom), which makes phosphorus very reactive to air. In fact, exfoliated flakes of black phosphorus are highly hygroscopic and tend to uptake moisture from air (*22*). Several initial studies report on quick water accumulation at the surface of exfoliated flakes (*23*–*29*). Figure 1 shows some examples from the literature of atomic force microscopy images of exfoliated black phosphorus flakes left in ambient conditions that progressively accumulates water with time (*22*, *26*, *27*).

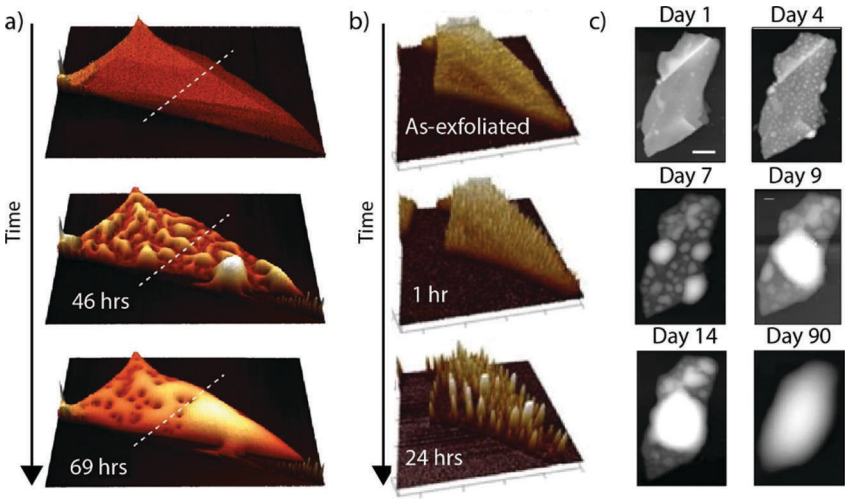

Figure 1. a)-c) Selected AFM scans of three BP flakes in air taken at different times after exfoliation. a) Adapted with permission from (*22*)*. Copyright 2015 IOP Publishing Ltd. b) Adapted with permission from* (*26*) *under a Creative Commons License (http://creativecommons.org/licenses/by/4.0/). c) Gamage, S.; Li, Z.; Yakovlev, V. S.; Lewis, C.; Wang, H.; Cronin, S. B.; Abate, Y. Nanoscopy of Black Phosphorus Degradation. Adv. Mater. Interfaces 2016, 3 (12), 1600121. Copyright Wiley-VCH Verlag GmbH & Co. KGaA. Reproduced with permission.*

Apart from the topographical changes induced by the moisture uptake of the black phosphorus flakes exposed to air, the environmental exposure also induces degradation of the optical, electrical and mechanical properties of black phosphorus. In fact, Favron *et al*. measured the evolution of the Raman intensity upon exposure to different atmospheres showing a clear degradation of black phosphorus in air (Figure 2a) (*28*).

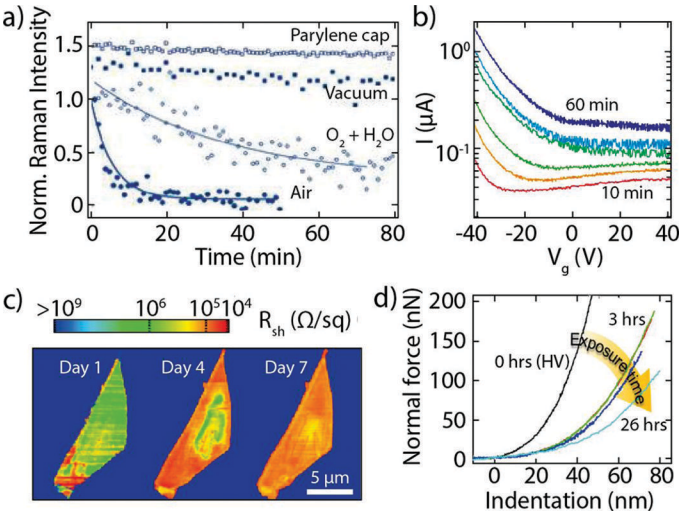

Figure 2. a) Integrated intensity of the A_g^2 Raman mode as a function of time under different exposure conditions: air, vacuum, O_2/H_2O mixture and 300 nm thick parylene layer-capped flake in air. The faster decay rate observed in air (5.5 min^{-1}) compared to under the O_2/H_2O mixture exposure (36 min^{-1}) is due to the photon flux (1.7 × 10^4 W cm^{-2} and 1.8 × 10^3 W cm^{-2}, respectively). Reproduced with permission from (28). Copyright 2015 Springer Nature. b) Transfer characteristics (IV_g) of a BP FET device at selected times over the first hour of exposure (curves are offset by 100 nA for clarity). Adapted with permission from (22). Copyright 2015 IOP Publishing Ltd. c) Local sheet resistance maps of a 24 nm thick flake capped by ~3 nm Al_2O_3 layer. Adapted with permission from (26) under a Creative Commons License (http://creativecommons.org/licenses/by/4.0/). d) F(δ) curves for a 5.3 nm thick BP drumhead in high vacuum and after 3, 7, 11 and 26 h of exposure to ambient conditions. Adapted with permission from (30) under a Creative Commons License (http://creativecommons.org/licenses/by/3.0/).

The electronic properties of black phosphorus are also strongly modified by the environmental exposure as illustrated by Island *et al*. and Wood *et al*. through direct electrical transport measurements as a function of the exposure in air (*22*, *25*) (see Figure 2b). Interestingly, from these transport measurements one can conclude that there are two different regimes: one at short-timescale where the modifications are mainly due to physisorption of O_2 and N_2 species and another one at longer timescales were the water absorption starts. In the short-timescale (less than 1 hour) there is an instant shift of the threshold voltage to the left (shown in Figure S6 (e) from the supplementary information file in ref. (*22*)) and an overall decrease in conductance and these changes are reversible by putting the device in vacuum. A vacuum to air zero bias resistance cycling experiment showed that during the first cycles up to the 7th, the initial value was recover (figure S4, from the supplementary information file in ref. (*22*)). At long-timescale the conductance of the devices steadily decreases until the device breakdown. Complementary to the macroscopic electrical transport measurements microscopic measurements with microwave impedance microscopy are a non-destructive, good asset to probe the effect of the environmental exposure on black phosphorus (*26*, *29*). As an example to illustrate the importance to study locally the mechanism of interaction between the BP surface and its degradation agents, figure 2c shows an example of a black phosphorus flake capped with a thin layer of Al_2O_3 that cannot effectively encapsulate completely the black

phosphorus flake (*26*). From the microwave impedance microscopy images one can conclude that the degradation process occurs first at the edges of the flake and then it is extended towards the center of the flake. This study allowed the authors to optimize the stability in air of the BP by capping it with a double layer of Al_2O_3/hydrophobic fluoropolymer film, instead of a single Al_2O_3 layer. Moreno-Moreno *et al*. demonstrated that exposing thin flakes of black phosphorus to air also degrades its mechanical properties: after 24 h or exposure to ambient the Young's modulus of thin black phosphorus flakes decreases by a factor of two (see Figure 2d) (*30*).

Regarding the physical and chemical mechanisms behind this environmental degradation of black phosphorus, Favron *et al*. and Zhou *et al*. have deduced that the degradation most likely occurs as a result of photo-induced oxidation from oxygen absorbed in accumulated water at the surface of exfoliated flakes exposed to ambient conditions. (*28*, *31*, *32*). Recently, Kim *et al*. have studied by scanning Kelvin probe microscopy (SKPM) the degradation process of black phosphorus in dark. They have observed that the degradation rate is layer-dependent, since the electronic structure of a 2D material changes with its thickness (*33*). Zhang *et al*. have combined experimental results and first-principle calculations to study the reaction kinetics of black phosphorus with oxygen contained in the water. They have concluded that the main products are the PO_2^{3-}, PO_3^{3-} and PO_4^{3-} species. They also showed the possibility to store BP in deoxygenated water under ambient light without degradation for at least 15 days (*34*). The exact role of water in the oxidation mechanism of the black phosphorus is not fully understood yet. As a consequence, further experimental results and theoretical models are being developed. A recent work has proposed that OH^- ions are responsible for the degradation of BP, through experimental observation and density functional theory calculations (DFT). They showed that the degradation of BP has therefore a dependence with the pH, with linear increasing degradation rate from pH 4 to 10 (*35*). Finally, Luo *et al*. studied the kinetics of black phosphorus oxidation under 5% O_2/Ar, 2.3% H_2O/Ar and 5% O_2/2.3% H_2O/Ar mixture. The highest rate of oxidation was found in the mixture of oxygen and water. The authors concluded that water continued to interact chemically with the oxidized BP surface promoting the oxygen dissociation further (*36*). The stepwise reactivity of H_2O with a phosphorene surface once it was oxidized was also studied theoretically (*37*).

Passivation Methods: Encapsulation and Functionalization

These works focused on the air-induced degradation of black phosphorus have motivated works to find effective methods to encapsulate black phosphorus at the early stages of isolation/fabrication to increase its longevity (*25*, *26*, *38*). Several encapsulation techniques have been reported to date including polymer dielectrics (*10*, *39*), atomic layer deposited (ALD) oxides (*25*, *26*, *40–42*), hybrid metal organic chemical vapor deposition (MOCVD)/ALD coating of BN/Al_2O_3 (*43*), electron-beam evaporated metallic thin films oxidized under ambient air (*44*), van der Waals heterostructures using boron nitride, MoS_2 and graphene flakes (*7–9*, *38*, *45–48*), and chemical functionalization (*49–52*). In two different works, a thin native oxide layer on top of the black phosphorus surface has been formed by oxygen plasma (*53*) or thermal annealing etching (*54*). In both works, the presence of the oxide proved to stop the degradation of BP. Tian *et al* have produced a thin native P_{ox} layer around 2 nm thick on the bottom side of black phosphorus films of typically 20 nm thick. This bottom oxide layer was formed under exposure in air for 30 min during the mechanical exfoliation

and metallic contacts deposition. The authors used the charge transfer induced at the bottom P_{ox}/BP interface to simulate synaptic behavior along the 45° angle spaced electrodes of a field-effect transistor, exploiting the in-plane anisotropy of the material. After fabrication and electrical measurements at vacuum, from room to high temperature, the devices were stored in a N_2 box under dark and the authors checked that the bottom oxide layer was not modified for a few months (*55*). Another work demonstrated the use of ozone generated by ultraviolet light under atmospheric pressure, to form phosphorus oxide on top of thick black phosphorus films. This oxide is etched away by rinsing with deionized water, leaving a thinner BP surface, which presents a retarded degradation effect in air. They found an etching rate of 12 ± 2 nm/h and could achieve a single-layer phosphorene film under this process (*56*).

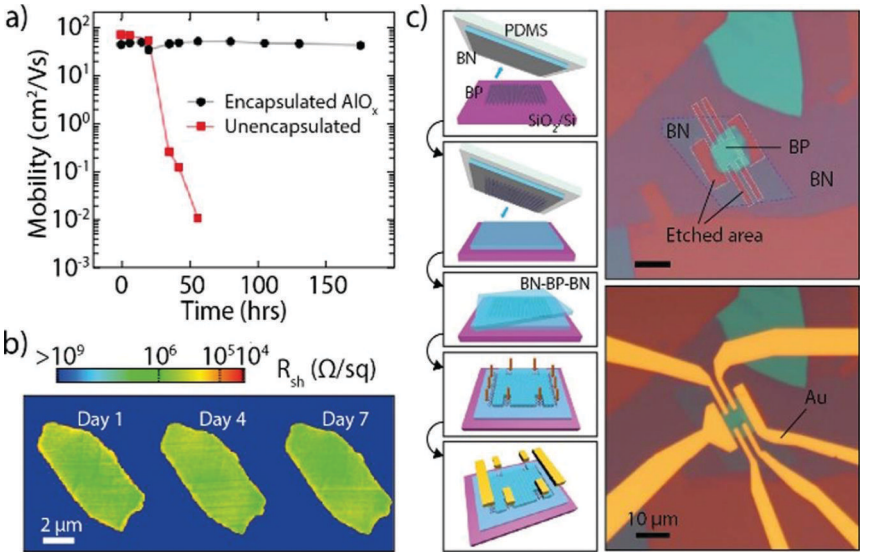

Figure 3. a) Hole mobility for encapsulated and unencapsulated BP FETs versus ambient exposure time. Reproduced with permission from (*25*)*. Copyright 2014 American Chemical Society. b) Sheet resistance maps of a 16 nm-thick flake capped by 25 nm Al_2O_3. Adapted with permission from* (*26*) *under a Creative Commons License (http://creativecommons.org/licenses/by/4.0/). c) (Left) Schematic of the BN–BP–BN heterostructure device fabrication process. (Right) Optical image of the BN–BP–BN heterostructure after O_2-plasma etching (the etched area is enclosed within the white line) and of the BN–BP–BN Hall-bar device. Adapted with permission from* (*47*) *under a Creative Commons License (http://creativecommons.org/licenses/by/4.0/).*

Figure 3a-b shows the results of encapsulating black phosphorus using a thick AlO_x capping layer (deposited through atomic layer deposition) (*25*, *26*). While uncapped field-effect transistors break down in a few days, field-effect transistors with encapsulation show performances (e.g. mobility and conductance) that do not change over several days (*25*). Microwave impedance microscopy measurement technique confirms that black phosphorus devices encapsulated with a thick AlO_x layer shows little to no degradation (*26*).

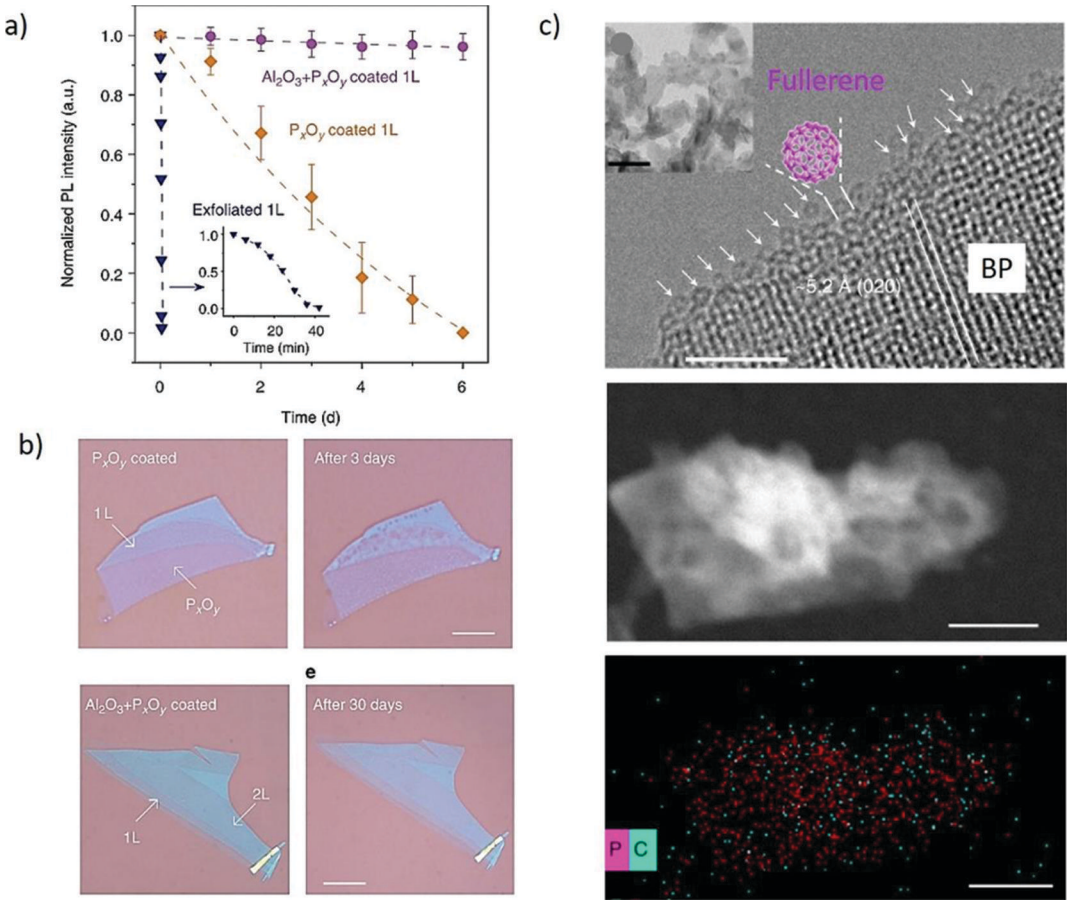

Figure 4. a) Time dependence of the normalized PL intensity of the monolayer phosphorene samples treated by different methods: exfoliated 1L phosphorene (red), 1L phosphorene with P_xO_y (~11 nm) capping layer produced by O_2 plasma etching (green) and 1L phosphorene with dual passivation layers of P_xO_y and 5 nm of ALD Al_2O_3 (black). All PL was measured in ambient condition under the same laser excitation. Inset: zoom in plot for the exfoliated 1L phosphorene sample. Adapted with permission from (53) *under a Creative Commons License (http://creativecommons.org/licenses/by/4.0/). b) Optical images of flakes covered by a thin P_xO_y layer and a Al_2O_3 + P_xO_y double layer after fabrication and respectively, after 3 days and 30 days. The images show the higher passivation effect of the double capping layer. Adapted with permission from* (53) *under a Creative Commons License (http://creativecommons.org/licenses/by/4.0/). c) HRTEM image of the hybrid structure, where the C_{60} molecules can be seen passivating the edges of the BP layer. Inset: low magnification TEM image (top). STEM image (middle) and EDX elemental mapping (bottom) of the C_{60}-BP hybrid structure to show the successful presence of the fullerenes along the borders. Adapted with permission from* (60) *under a Creative Commons License (http://creativecommons.org/licenses/by/4.0/).*

Sandwiching black phosphorus flakes between boron nitride flakes (bottom and top encapsulation, see Figure 3c) is a more advanced route toward passivation which has proven to be a method to obtain exquisite electronic properties for graphene and MoS_2 devices. This enhancement of the device performance is due to the atomically flat, dangling-bond-free and defect free surface of hexagonal boron nitride (*47*, *57*, *58*). Thanks to this improved performance in these fully

encapsulated devices it has been possible to observe interesting physical phenomena not observable in low-mobility electronic devices such as the Shubnikov-de Haas oscillations and the integer quantum Hall effect (*7*–*9*, *46*, *47*). Figure 4a) shows the passivation effects of a P_xO_y layer formed by an oxygen plasma to thin down the initial exfoliated thick phosphorene layer (orange curve). This oxide layer was found to have a dual passivation role: its presence itself slowed down the degradation rate under ambient exposure. Then, for a dual passivation process depositing further a Al_2O_3 layer by ALD to increase the lifetime of the device, the oxide served as a protection layer to prevent the reaction of the phosphorene with the ALD precursors (pink curve) The optical images reinforce the longer time stability of double capped flakes compared to one that was also covered by the oxide layer (*53*).

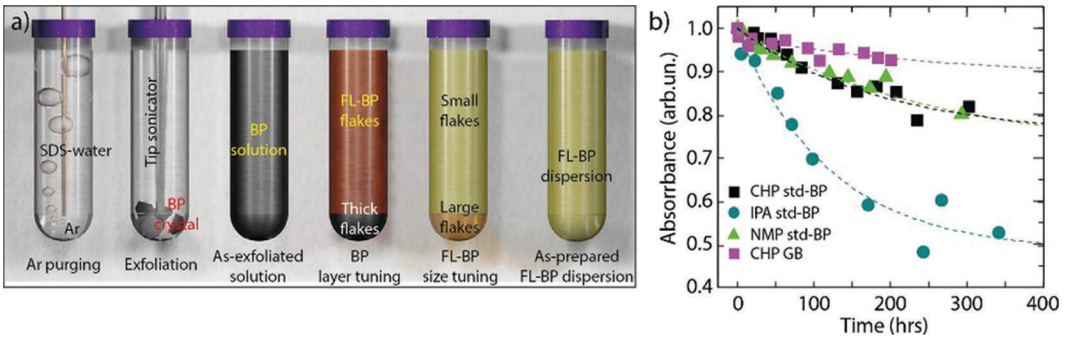

Figure 5. a) Preparation process to obtain few-layer phosphorene enriched aqueous dispersions. The workflow is represented by the test tubes, going the order of the different steps from left to right. Deoxygenated water with 2% (wt/vol) SDS was prepared by ultrahigh-purity Ar purging. The exfoliation of the BP crystal was performed in a sealed container using tip ultrasonication. Then, this solution was centrifuged to remove unexfoliated BP crystals. The remaining FL-BP dispersion was ultracentrifuged to precipitate large flakes. The supernatant was finally redispersed in deoxygenated water. Reproduced with permission from (67). Copyright 2016 National Academy of Sciences. b) Relative absorbance as a function of time, measured at 465 nm for: the standard few-layer BP dispersion exfoliated in CHP, in NMP, in IPA and the BP exfoliated in CHP in a glovebox (CHP GB). Adapted with permission from (66) under a Creative Commons License (http://creativecommons.org/licenses/by/4.0/).

Another strategy pursued to improve the stability of the black phosphorus under ambient conditions and consequently, its performance as device is the functionalization of its surface with different elements and molecules. The adsorption of Ag^+ ions on the black phosphorus surface via cation-π interactions constitutes an example of such approach. To produce such metal ion modified surface, a mechanically exfoliated BP flake transferred to a 300 nm SiO_2/Si substrate was immersed in a N-methyl-2-pyrrolidine (NMP) solution with silver nitrate ($1x10^{-6}$ M). They observed an improvement on the hole mobility from 796 to 1593 cm^2/V s and the ON/OFF ratio from $5.9x10^4$ to $2.5x10^6$ after 1 h immersion, compared to the original device before passivation (*59*). In another work, the edges of BP nanosheets were functionalized by covalent bonding with C_{60} molecules (see Figure 4c). The fullerenes were chosen due to its high hydrophobicity. These C_{60} functionalized black phosphorus films showed higher stability against oxidation and good photocurrent characteristics (*60*). The functionalization of a black phosphorus surface with antioxidant molecules following processes such as fluorination (*61*) or treatment in imidazolium-based ionic liquids (*62*)

were pursued. A sulfur doped thin layer BP field effect transistor showed around 77% of the mobility and an I_{ON}/I_{OFF} ratio of 10^3 still after 21 days under ambient exposure (*63*). Aluminum doped black phosphorus flakes were used to produce FETs that presented an n-doping effect and unnoticeable degradation after 10 days under ambient conditions (*64*). Finally, density functional theory calculations were performed to estimate the ratio of BP doping with scandium atoms at which the flake was protected from the oxygen and water molecules, but also retained the semiconductor behavior (*65*).

An alternative approach to address the environmental instability issue consists on using liquid phase exfoliation to obtain suspensions of black phosphorus nanosheets. It has been demonstrated that liquid phase exfoliation can produce large quantities of high-quality few-layer black phosphorus nanosheets. These black phosphorus nanosheets are surprisingly stable in suspension (even when deoxygenated water is used as solvent for the liquid phase exfoliation), probably due to the solvation shell protecting the nanosheets from reacting with oxygen (Figure 5) (*66–71*).

In summary, in this chapter we have discussed the issue of the environmental instability in black phosphorus and the works devoted to develop strategies to effectively encapsulate black phosphorus to preserve its pristine properties.

References

1. Li, L.; Yu, Y.; Ye, G. J.; Chen, X. H.; Zhang, Y. Electronic Properties of Few-Layer Black Phosphorus. *Bull. Am. Phys. Soc.* **2013**, *58*.
2. Bridgman, P. W. Two New Modifications of Phosphorus. *J. Am. Chem. Soc.* **1914**, *36* (7), 1344–1363. https://doi.org/10.1021/ja02184a002.
3. Keyes, R. W. The Electrical Properties of Black Phosphorus. *Phys. Rev.* **1953**, *92* (3), 580–584. https://doi.org/10.1103/PhysRev.92.580.
4. Li, L.; Yu, Y.; Ye, G. J.; Ge, Q.; Ou, X.; Wu, H.; Feng, D.; Chen, X. H.; Zhang, Y. Black Phosphorus Field-Effect Transistors. *Nat. Nanotechnol.* **2014**, *9* (5), 372–377. https://doi.org/10.1038/nnano.2014.35.
5. Xia, F.; Wang, H.; Jia, Y. Rediscovering Black Phosphorus as an Anisotropic Layered Material for Optoelectronics and Electronics. *Nat. Commun.* **2014**, *5*. https://doi.org/10.1038/ncomms5458.
6. Liu, H.; Neal, A. T.; Zhu, Z.; Luo, Z.; Xu, X.; Tománek, D.; Ye, P. D. Phosphorene: An Unexplored 2D Semiconductor with a High Hole Mobility. *ACS Nano* **2014**, *8* (4), 4033–4041. https://doi.org/10.1021/nn501226z.
7. Li, L.; Yang, F.; Ye, G. J.; Zhang, Z.; Zhu, Z.; Lou, W.; Zhou, X.; Li, L.; Watanabe, K.; Taniguchi, T.; et al. Quantum Hall Effect in Black Phosphorus Two-Dimensional Electron System. *Nat. Nanotechnol.* **2016**, *11* (7), 593–597. https://doi.org/10.1038/nnano.2016.42.
8. Li, L.; Ye, G. J.; Tran, V.; Fei, R.; Chen, G.; Wang, H.; Wang, J.; Watanabe, K.; Taniguchi, T.; Yang, L.; et al. Quantum Oscillations in a Two-Dimensional Electron Gas in Black Phosphorus Thin Films. *Nat. Nanotechnol.* **2015**, *10* (7), 608–613. https://doi.org/10.1038/nnano.2015.91.
9. Gillgren, N.; Wickramaratne, D.; Shi, Y.; Espiritu, T.; Yang, J.; Hu, J.; Wei, J.; Liu, X.; Mao, Z.; Watanabe, K.; et al. Gate Tunable Quantum Oscillations in Air-Stable and High Mobility

Few-Layer Phosphorene Heterostructures. *2D Mater.* **2014**, *2* (1), 011001. https://doi.org/10.1088/2053-1583/2/1/011001.
10. Engel, M.; Steiner, M.; Avouris, P. Black Phosphorus Photodetector for Multispectral, High-Resolution Imaging. *Nano Lett.* **2014**, *14* (11), 6414–6417. https://doi.org/10.1021/nl502928y.
11. Youngblood, N.; Chen, C.; Koester, S. J.; Li, M. Waveguide-Integrated Black Phosphorus Photodetector with High Responsivity and Low Dark Current. *Nat. Photonics* **2015**, *9* (4), 247–252. https://doi.org/10.1038/nphoton.2015.23.
12. Buscema, M.; Groenendijk, D. J.; Blanter, S. I.; Steele, G. A.; Van Der Zant, H. S. J.; Castellanos-Gomez, A. Fast and Broadband Photoresponse of Few-Layer Black Phosphorus Field-Effect Transistors. *Nano Lett.* **2014**, *14* (6) https://doi.org/10.1021/nl5008085.
13. Yuan, H.; Liu, X.; Afshinmanesh, F.; Li, W.; Xu, G.; Sun, J.; Lian, B.; Curto, A. G.; Ye, G.; Hikita, Y.; et al. Polarization-Sensitive Broadband Photodetector Using a Black Phosphorus Vertical p-n Junction. *Nat. Nanotechnol.* **2015**, *10* (8), 707–713. https://doi.org/10.1038/nnano.2015.112.
14. Yuan, H.; Liu, X.; Afshinmanesh, F.; Li, W.; Xu, G.; Sun, J.; Lian, B.; Ye, G.; Hikita, Y.; Shen, Z.; et al. *Broadband Linear-Dichroic Photodetector in a Black Phosphorus Vertical p-n Junction*. 2014, arXiv:1409.4729 [cond-mat.mes-hall]. arXiv.org e-Print archive. https://arxiv.org/abs/1409.4729.
15. Guo, Q.; Pospischil, A.; Bhuiyan, M.; Jiang, H.; Tian, H.; Farmer, D.; Deng, B.; Li, C.; Han, S. J.; Wang, H.; et al. Black Phosphorus Mid-Infrared Photodetectors with High Gain. *Nano Lett.* **2016**, *16* (7), 4648–4655. https://doi.org/10.1021/acs.nanolett.6b01977.
16. Chen, X.; Lu, X.; Deng, B.; Sinai, O.; Shao, Y.; Li, C.; Yuan, S.; Tran, V.; Watanabe, K.; Taniguchi, T.; et al. Widely Tunable Black Phosphorus Mid-Infrared Photodetector. *Nat. Commun.* **2017**, *8* (1) https://doi.org/10.1038/s41467-017-01978-3.
17. Abate, Y.; Akinwande, D.; Gamage, S.; Wang, H.; Snure, M.; Poudel, N.; Cronin, S. B. Recent Progress on Stability and Passivation of Black Phosphorus. *Advanced Materials* **2018**, 30 (29). https://doi.org/10.1002/adma.201704749.
18. Kuriakose, S.; Ahmed, T.; Balendhran, S.; Bansal, V.; Sriram, S.; Bhaskaran, M.; Walia, S. Black Phosphorus: Ambient Degradation and Strategies for Protection. *2D Materials* **2018**, 5. https://doi.org/10.1088/2053-1583/aab810.
19. Li, Q.; Zhou, Q.; Shi, L.; Chen, Q.; Wang, J. Recent Advances in Oxidation and Degradation Mechanisms of Ultrathin 2D Materials under Ambient Conditions and Their Passivation Strategies. *Journal of Materials Chemistry A* **2019**, 7, 4291–4312. https://doi.org/10.1039/c8ta10306b.
20. Kulish, V. V.; Malyi, O. I.; Persson, C.; Wu, P. Adsorption of Metal Adatoms on Single-Layer Phosphorene. *Phys. Chem. Chem. Phys.* **2015**, *17* (2), 992–1000. https://doi.org/10.1039/c4cp03890h.
21. Ziletti, A.; Carvalho, A.; Campbell, D. K.; Coker, D. F.; Castro Neto, A. H. Oxygen Defects in Phosphorene. *Phys. Rev. Lett.* **2015**, *114* (4) https://doi.org/10.1103/PhysRevLett.114.046801.
22. Island, J. O.; Steele, G. A.; Van Der Zant, H. S. J.; Castellanos-Gomez, A. Environmental Instability of Few-Layer Black Phosphorus. *2D Mater.* **2015**, *2* (1) https://doi.org/10.1088/2053-1583/2/1/011002.

23. Castellanos-Gomez, A.; Vicarelli, L.; Prada, E.; Island, J. O.; Narasimha-Acharya, K. L.; Blanter, S. I.; Groenendijk, D. J.; Buscema, M.; Steele, G. A.; Alvarez, J. V.; et al. Isolation and Characterization of Few-Layer Black Phosphorus. *2D Mater.* **2014**, *1* (2) https://doi.org/10.1088/2053-1583/1/2/025001.
24. Koenig, S. P.; Doganov, R. A.; Schmidt, H.; Castro Neto, A. H.; Özyilmaz, B. Electric Field Effect in Ultrathin Black Phosphorus. *Appl. Phys. Lett.* **2014**, *104* (10) https://doi.org/10.1063/1.4868132.
25. Wood, J. D.; Wells, S. A.; Jariwala, D.; Chen, K.-S.; Cho, E.; Sangwan, V. K.; Liu, X.; Lauhon, L. J.; Marks, T. J.; Hersam, M. C. Effective Passivation of Exfoliated Black Phosphorus Transistors against Ambient Degradation. *Nano Lett.* **2014**, *14* (12), 6964–6970. https://doi.org/10.1021/nl5032293.
26. Kim, J. S.; Liu, Y.; Zhu, W.; Kim, S.; Wu, D.; Tao, L.; Dodabalapur, A.; Lai, K.; Akinwande, D. Toward Air-Stable Multilayer Phosphorene Thin-Films and Transistors. *Sci. Rep.* **2015**, *5*. https://doi.org/10.1038/srep08989.
27. Gamage, S.; Li, Z.; Yakovlev, V. S.; Lewis, C.; Wang, H.; Cronin, S. B.; Abate, Y. Nanoscopy of Black Phosphorus Degradation. *Adv. Mater. Interfaces* **2016**, *3* (12), 1600121. https://doi.org/10.1002/admi.201600121.
28. Favron, A.; Gaufrès, E.; Fossard, F.; Phaneuf-Laheureux, A. L.; Tang, N. Y. W.; Lévesque, P. L.; Loiseau, A.; Leonelli, R.; Francoeur, S.; Martel, R. Photooxidation and Quantum Confinement Effects in Exfoliated Black Phosphorus. *Nat. Mater.* **2015**, *14* (8), 826–832. https://doi.org/10.1038/nmat4299.
29. De Visser, P. J.; Chua, R.; Island, J. O.; Finkel, M.; Katan, A. J.; Thierschmann, H.; Van Der Zant, H. S. J.; Klapwijk, T. M. Spatial Conductivity Mapping of Unprotected and Capped Black Phosphorus Using Microwave Microscopy. *2D Mater.* **2016**, *3* (2) https://doi.org/10.1088/2053-1583/3/2/021002.
30. Moreno-Moreno, M.; Lopez-Polin, G.; Castellanos-Gomez, A.; Gomez-Navarro, C.; Gomez-Herrero, J. Environmental Effects in Mechanical Properties of Few-Layer Black Phosphorus. *2D Mater.* **2016**, *3* (3) https://doi.org/10.1088/2053-1583/3/3/031007.
31. Zhou, Q.; Chen, Q.; Tong, Y.; Wang, J. Light-induced Ambient Degradation of Few-layer Black Phosphorus: Mechanism and Protection. *Angew. Chemie Int. Ed.* **2016**, *55* (38), 11437–11441.
32. Huang, Y.; Qiao, J.; He, K.; Bliznakov, S.; Sutter, E.; Chen, X.; Luo, D.; Meng, F.; Su, D.; Decker, J.; et al. Interaction of Black Phosphorus with Oxygen and Water. *Chem. Mater.* **2016**, *28* (22), 8330–8339. https://doi.org/10.1021/acs.chemmater.6b03592.
33. Kim, M.; Kim, H.-g.; Park, S.; Kim, J. S.; Choi, H. J.; Im, S.; Lee, H.; Kim, T.; Yi, Y. Intrinsic Correlation between Electronic Structure and Degradation: From Few-Layer to Bulk Black Phosphorus. *Angew. Chemie - Int. Ed.* **2019**, *58* (12), 3754–3758. https://doi.org/10.1002/anie.201811743.
34. Zhang, T.; Wan, Y.; Xie, H.; Mu, Y.; Du, P.; Wang, D.; Wu, X.; Ji, H.; Wan, L. Degradation Chemistry and Stabilization of Exfoliated Few-Layer Black Phosphorus in Water. *J. Am. Chem. Soc.* **2018**, *140* (24), 7561–7567. https://doi.org/10.1021/jacs.8b02156.
35. Zhang, S.; Zhang, X.; Lei, L.; Yu, X. F.; Chen, J.; Ma, C.; Wu, F.; Zhao, Q.; Xing, B. pH-Dependent Degradation of Layered Black Phosphorus: Essential Role of Hydroxide Ions. *Angew. Chemie - Int. Ed.* **2019**, *58* (2), 467–471. https://doi.org/10.1002/anie.201809989.

36. Luo, W.; Zemlyanov, D. Y.; Milligan, C. A.; Du, Y.; Yang, L.; Wu, Y.; Ye, P. D. Surface Chemistry of Black Phosphorus under a Controlled Oxidative Environment. *Nanotechnology* **2016**, *27* (43) https://doi.org/10.1088/0957-4484/27/43/434002.
37. Wang, G.; Slough, W. J.; Pandey, R.; Karna, S. P. Degradation of Phosphorene in Air: Understanding at Atomic Level. *2D Mater.* **2016**, *3* (2) https://doi.org/10.1088/2053-1583/3/2/025011.
38. Avsar, A.; Vera-Marun, I. J.; Tan, J. Y.; Watanabe, K.; Taniguchi, T.; Castro Neto, A. H.; Özyilmaz, B. Air-Stable Transport in Graphene-Contacted, Fully Encapsulated Ultrathin Black Phosphorus-Based Field-Effect Transistors. *ACS Nano* **2015**, *9* (4), 4138–4145. https://doi.org/10.1021/acsnano.5b00289.
39. Tayari, V.; Hemsworth, N.; Fakih, I.; Favron, A.; Gaufrès, E.; Gervais, G.; Martel, R.; Szkopek, T. Two-Dimensional Magnetotransport in a Black Phosphorus Naked Quantum Well. *Nat. Commun.* **2015**, *6*, 7702. https://doi.org/10.1038/ncomms8702.
40. Na, J.; Lee, Y. T.; Lim, J. A.; Hwang, D. K.; Kim, G.-T.; Choi, W. K.; Song, Y.-W. Few-Layer Black Phosphorus Field-Effect Transistors with Reduced Current Fluctuation. *ACS Nano* **2014**, *8* (11), 11753–11762. https://doi.org/10.1021/nn5052376.
41. Zhu, W.; Yogeesh, M. N.; Yang, S.; Aldave, S. H.; Kim, J. S.; Sonde, S.; Tao, L.; Lu, N.; Akinwande, D. Flexible Black Phosphorus Ambipolar Transistors, Circuits and AM Demodulator. *Nano Lett.* **2015**, *15* (3), 1883–1890. https://doi.org/10.1021/nl5047329.
42. Illarionov, Y. Y.; Waltl, M.; Rzepa, G.; Knobloch, T.; Kim, J.-S.; Akinwande, D.; Grasser, T. Highly-Stable Black Phosphorus Field-Effect Transistors with Low Density of Oxide Traps. *npj 2D Mater. Appl.* **2017**, *1* (1) https://doi.org/10.1038/s41699-017-0025-3.
43. Gamage, S.; Fali, A.; Aghamiri, N.; Yang, L.; Ye, P. D.; Abate, Y. Reliable Passivation of Black Phosphorus by Thin Hybrid Coating. *Nanotechnology* **2017**, *28* (26) https://doi.org/10.1088/1361-6528/aa7532.
44. Wu, D.; Peng, Z.; Jin, C.; Zhang, Z. Effective Passivation of Black Phosphorus Transistor against Ambient Degradation by an Ultra-Thin Tin Oxide Film. *Sci. Bull.* **2019**, *64* (9), 570–574. https://doi.org/10.1016/j.scib.2019.04.021.
45. Doganov, R. A.; O'Farrell, E. C. T.; Koenig, S. P.; Yeo, Y.; Ziletti, A.; Carvalho, A.; Campbell, D. K.; Coker, D. F.; Watanabe, K.; Taniguchi, T.; et al. Transport Properties of Pristine Few-Layer Black Phosphorus by van Der Waals Passivation in an Inert Atmosphere. *Nat. Commun.* **2015**, *6*. https://doi.org/10.1038/ncomms7647.
46. Cao, Y.; Mishchenko, A.; Yu, G. L.; Khestanova, E.; Rooney, A. P.; Prestat, E.; Kretinin, A. V.; Blake, P.; Shalom, M. B.; Woods, C.; et al. Quality Heterostructures from Two Dimensional Crystals Unstable in Air by Their Assembly in Inert Atmosphere. *Nano Lett.* **2015**, *15* (8), 4914–4921. https://doi.org/10.1021/acs.nanolett.5b00648.
47. Chen, X.; Wu, Y.; Wu, Z.; Han, Y.; Xu, S.; Wang, L.; Ye, W.; Han, T.; He, Y.; Cai, Y.; et al. High-Quality Sandwiched Black Phosphorus Heterostructure and Its Quantum Oscillations. *Nat. Commun.* **2015**, *6*. https://doi.org/10.1038/ncomms8315.
48. Son, Y.; Kozawa, D.; Liu, A. T.; Koman, V. B.; Wang, Q. H.; Strano, M. S. A Study of Bilayer Phosphorene Stability under MoS2-Passivation. *2D Mater.* **2017**, *4* (2) https://doi.org/10.1088/2053-1583/aa6e35.

49. Ryder, C. R.; Wood, J. D.; Wells, S. A.; Yang, Y.; Jariwala, D.; Marks, T. J.; Schatz, G. C.; Hersam, M. C. Covalent Functionalization and Passivation of Exfoliated Black Phosphorus via Aryl Diazonium Chemistry. *Nat. Chem.* **2016**, *8* (6), 597–602. https://doi.org/10.1038/nchem.2505.
50. Abellán, G.; Lloret, V.; Mundloch, U.; Marcia, M.; Neiss, C.; Görling, A.; Varela, M.; Hauke, F.; Hirsch, A. Noncovalent Functionalization of Black Phosphorus. *Angew. Chemie - Int. Ed.* **2016**, *55* (47), 14557–14562. https://doi.org/10.1002/anie.201604784.
51. Zhao, Y.; Wang, H.; Huang, H.; Xiao, Q.; Xu, Y.; Guo, Z.; Xie, H.; Shao, J.; Sun, Z.; Han, W.; et al. Surface Coordination of Black Phosphorus for Robust Air and Water Stability. *Angew. Chemie - Int. Ed.* **2016**, *55* (16), 5003–5007. https://doi.org/10.1002/anie.201512038.
52. Yue, D.; Lee, D.; Jang, Y. D.; Choi, M. S.; Nam, H. J.; Jung, D. Y.; Yoo, W. J. Passivated Ambipolar Black Phosphorus Transistors. *Nanoscale* **2016**, *8* (25), 12773–12779. https://doi.org/10.1039/c6nr02554d.
53. Pei, J.; Gai, X.; Yang, J.; Wang, X.; Yu, Z.; Choi, D. Y.; Luther-Davies, B.; Lu, Y. Producing Air-Stable Monolayers of Phosphorene and Their Defect Engineering. *Nat. Commun.* **2016**, *7*. https://doi.org/10.1038/ncomms10450.
54. Jeong, M. H.; Kwak, D. H.; Ra, H. S.; Lee, A. Y.; Lee, J. S. Realizing Long-Term Stability and Thickness Control of Black Phosphorus by Ambient Thermal Treatment. *ACS Appl. Mater. Interfaces* **2018**, *10* (22), 19069–19075. https://doi.org/10.1021/acsami.8b04627.
55. Tian, H.; Guo, Q.; Xie, Y.; Zhao, H.; Li, C.; Cha, J. J.; Xia, F.; Wang, H. Anisotropic Black Phosphorus Synaptic Device for Neuromorphic Applications. *Adv. Mater.* **2016**, *28* (25), 4991–4997. https://doi.org/10.1002/adma.201600166.
56. Kwon, H.; Seo, S. W.; Kim, T. G.; Lee, E. S.; Lanh, P. T.; Yang, S.; Ryu, S.; Kim, J. W. Ultrathin and Flat Layer Black Phosphorus Fabricated by Reactive Oxygen and Water Rinse. *ACS Nano* **2016**, *10* (9), 8723–8731. https://doi.org/10.1021/acsnano.6b04194.
57. Wang, L.; Meric, I.; Huang, P. Y.; Gao, Q.; Gao, Y.; Tran, H.; Taniguchi, T.; Watanabe, K.; Campos, L. M.; Muller, D. A.; et al. One-Dimensional Electrical Contact to a Two-Dimensional Material. *Science (80-.).* **2013**, *342* (6158), 614–617. https://doi.org/10.1126/science.1244358.
58. Cui, X.; Lee, G. H.; Kim, Y. D.; Arefe, G.; Huang, P. Y.; Lee, C. H.; Chenet, D. A.; Zhang, X.; Wang, L.; Ye, F.; et al. Multi-Terminal Transport Measurements of MoS 2 Using a van Der Waals Heterostructure Device Platform. *Nat. Nanotechnol.* **2015**, *10* (6), 534–540. https://doi.org/10.1038/nnano.2015.70.
59. Guo, Z.; Chen, S.; Wang, Z.; Yang, Z.; Liu, F.; Xu, Y.; Wang, J.; Yi, Y.; Zhang, H.; Liao, L.; et al. Metal-Ion-Modified Black Phosphorus with Enhanced Stability and Transistor Performance. *Adv. Mater.* **2017**, *29* (42) https://doi.org/10.1002/adma.201703811.
60. Zhu, X.; Zhang, T.; Jiang, D.; Duan, H.; Sun, Z.; Zhang, M.; Jin, H.; Guan, R.; Liu, Y.; Chen, M.; et al. Stabilizing Black Phosphorus Nanosheets via Edge-Selective Bonding of Sacrificial C 60 Molecules. *Nat. Commun.* **2018**, *9* (1) https://doi.org/10.1038/s41467-018-06437-1.
61. Tang, X.; Liang, W.; Zhao, J.; Li, Z.; Qiu, M.; Fan, T.; Luo, C. S.; Zhou, Y.; Li, Y.; Guo, Z.; et al. Fluorinated Phosphorene: Electrochemical Synthesis, Atomistic Fluorination, and Enhanced Stability. *Small* **2017**, *13* (47) https://doi.org/10.1002/smll.201702739.
62. Walia, S.; Balendhran, S.; Ahmed, T.; Singh, M.; El-Badawi, C.; Brennan, M. D.; Weerathunge, P.; Karim, M. N.; Rahman, F.; Rassell, A.; et al. Ambient Protection of Few-

Layer Black Phosphorus via Sequestration of Reactive Oxygen Species. *Adv. Mater.* **2017**, *29* (27) https://doi.org/10.1002/adma.201700152.

63. Lv, W.; Yang, B.; Wang, B.; Wan, W.; Ge, Y.; Yang, R.; Hao, C.; Xiang, J.; Zhang, B.; Zeng, Z.; et al. Sulfur-Doped Black Phosphorus Field-Effect Transistors with Enhanced Stability. *ACS Appl. Mater. Interfaces* **2018**, *10* (11), 9663–9668. https://doi.org/10.1021/acsami.7b19169.
64. Wang, Z.; Lu, J.; Wang, J.; Li, J.; Du, Z.; Wu, H.; Liao, L.; Chu, P. K.; Yu, X. F. Air-Stable n-Doped Black Phosphorus Transistor by Thermal Deposition of Metal Adatoms. *Nanotechnology* **2019**, *30* (13) https://doi.org/10.1088/1361-6528/aafd68.
65. Wang, X.; Tang, C.; Zhu, W.; Zhou, X.; Zhou, Q.; Cheng, C. A New Effective Approach to Prevent the Degradation of Black Phosphorus: The Scandium Transition Metal Doping. *J. Phys. Chem. C* **2018**, *122* (17), 9654–9662. https://doi.org/10.1021/acs.jpcc.8b01089.
66. Hanlon, D.; Backes, C.; Doherty, E.; Cucinotta, C. S.; Berner, N. C.; Boland, C.; Lee, K.; Harvey, A.; Lynch, P.; Gholamvand, Z.; et al. Liquid Exfoliation of Solvent-Stabilized Few-Layer Black Phosphorus for Applications beyond Electronics. *Nat. Commun.* **2015**, *6*. https://doi.org/10.1038/ncomms9563.
67. Kang, J.; Wells, S. A.; Wood, J. D.; Lee, J.-H.; Liu, X.; Ryder, C. R.; Zhu, J.; Guest, J. R.; Husko, C. A.; Hersam, M. C. Stable Aqueous Dispersions of Optically and Electronically Active Phosphorene. *Proc. Natl. Acad. Sci.* **2016**, *113* (42), 11688–11693. https://doi.org/10.1073/pnas.1602215113.
68. Kang, J.; Wood, J. D.; Wells, S. A.; Lee, J. H.; Liu, X.; Chen, K. S.; Hersam, M. C. Solvent Exfoliation of Electronic-Grade, Two-Dimensional Black Phosphorus. *ACS Nano* **2015**, *9* (4), 3596–3604. https://doi.org/10.1021/acsnano.5b01143.
69. Yasaei, P.; Kumar, B.; Foroozan, T.; Wang, C.; Asadi, M.; Tuschel, D.; Indacochea, J. E.; Klie, R. F.; Salehi-Khojin, A. High-Quality Black Phosphorus Atomic Layers by Liquid-Phase Exfoliation. *Adv. Mater.* **2015**, *27* (11), 1887–1892. https://doi.org/10.1002/adma.201405150.
70. Chaban, V. V.; Fileti, E. E.; Prezhdo, O. V. Imidazolium Ionic Liquid Mediates Black Phosphorus Exfoliation While Preventing Phosphorene Decomposition. *ACS Nano* **2017**, *11* (6), 6459–6466. https://doi.org/10.1021/acsnano.7b03074.
71. Li, Q.; Zhao, Y.; Guo, J.; Zhou, Q.; Chen, Q.; Wang, J. On-Surface Synthesis: A Promising Strategy toward the Encapsulation of Air Unstable Ultra-Thin 2D Materials. *Nanoscale* **2018**, *10* (8), 3799–3804. https://doi.org/10.1039/c7nr09178h.